applied sciences

MDPI

Article

Identification and Characterization of a Novel Thermostable GDSL Lipase LipGt6 from *Geobacillus thermoleovorans* H9

Lirong Qin [1,2,3], Min Lin [1,2,3], Yuhua Zhan [2,3], Shijie Jiang [1], Zhengfu Zhou [2,3,*] and Jin Wang [1,2,3,*]

[1] College of Life Science and Engineering, Southwest University of Science and Technology, Mianyang 621000, China; qinlirong0906@163.com (L.Q.); linmin@caas.cn (M.L.); sjjiang0406@swust.edu.cn (S.J.)
[2] National Key Laboratory of Agricultural Microbiology, Biotechnology Research Institute, Chinese Academy of Agricultural Sciences, Beijing 100081, China; zhanyuhua@caas.cn
[3] Key Laboratory of Agricultural Microbiome (MARA), Biotechnology Research Institute, Chinese Academy of Agricultural Sciences, Beijing 100081, China
* Correspondence: zhouzhengfu@caas.cn (Z.Z.); wangjin@caas.cn (J.W.)

Abstract: Lipases are versatile biocatalysts for various biological reactions. In the detergent industry, lipases must exhibit high activity in environments with high temperature, high pH values, metal ions, and organic solvents. Therefore, researchers are intensively searching for more stable and efficient lipases. A new thermophilic lipase, LipGt6, was identified in *Geobacillus thermoleovorans* H9, a new thermophilic strain isolated from ultrahigh-temperature compost. A structural model of LipGt6 was constructed using an esterase from *Geobacillus thermodenitrificans* as a template, and site-directed mutagenesis confirmed the predicted active site residues. LipGt6 exhibited the highest activity towards medium- and long-chain fatty acids (C8–C14), and the optimum temperature and pH were 50 °C and 9.0, respectively. LipGt6 was found to be thermostable up to 70 °C. In the presence of 1% H_2O_2 and sodium deoxycholate, LipGt6 retained 70 to 75% relative activity. These findings reveal that LipGt6 is potentially useful for the industrial production of detergent. Based on comparison of the amino acid sequences, the enzyme belongs to a new subfamily called lipolytic enzyme family II. The catalytic residues Ser and His were more critical than Asp, and the Asp221 catalytic residue is not likely critical for the lipolytic reaction of LipGt6.

Keywords: *Geobacillus thermoleovorans*; GDSL lipase; LipGt6; thermostable

Citation: Qin, L.; Lin, M.; Zhan, Y.; Jiang, S.; Zhou, Z.; Wang, J. Identification and Characterization of a Novel Thermostable GDSL Lipase LipGt6 from *Geobacillus thermoleovorans* H9. *Appl. Sci.* **2024**, *14*, 3279. https://doi.org/10.3390/app14083279

Received: 15 March 2024
Revised: 5 April 2024
Accepted: 11 April 2024
Published: 13 April 2024

1. Introduction

Lipases (EC3.1.1.3) belong to the family of lipolytic enzymes that perform hydrolysis and esterification of triacylglycerides and other water-insoluble esters [1]. Lipases are widely used in the detergent, food, dairy, pulp, and pharmaceutical industries because they possess a conserved catalytic triad structure, are stable in organic solvents, undergo interfacial activation in microaqueous environments, and exhibit high substrate specificity [2]. Based on amino acid sequence homology and fundamental biological properties, bacterial lipolytic enzymes have been classified into eight families [3]. Family II, also known as the GDSL family, has five consensus sequences (I–V) and four invariant important catalytic residues (Ser, Gly, Asn, and His in blocks I, II, III, and V, respectively). Ser residues are near the N-terminal end of the amino acid sequence [4]. To date, there have been few reports of GDSL family lipases in bacteria.

Many different gram-positive and gram-negative bacterial strains produce lipases. Some of the most commercially important bacteria that produce lipases are *Bacillus* sp., *Pseudomonas* sp., and *Burkholderia* sp. [5–7]. These microbial lipases operate at a wider temperature range, and their stability and activity are greater. The reported lipase from *Bacillus thermoleovorans* ID-1 showed optimal activity at 70–75 °C and pH 7.5 and extracellular lipase activity on a variety of lipid substrates at elevated temperatures. This lipase

has been applied in the biological treatment of oily wastewater [8]. In addition, researchers found that BL1 was active over a wide range of pH values (from 9.0 to 13.0), with an optimum pH of 11.0, and exhibited maximal activity at 55 °C. The enzyme showed excellent stability and compatibility with various commercial detergents [9]. Lipases have a wide range of industrial applications, and the detergent industry is an important field for the application of lipases. However, few lipases are currently used in the detergent industry.

Therefore, more stable and efficient alkaline lipases need to be identified from nature. Thermophilic bacteria are potential sources of thermostable alkaline lipases. High-temperature compost can reach as high as 80 °C in the ultrahigh-temperature phase, and the microbial community tends to be homogeneous. The dominant bacteria are mainly *Saccharomonospora* (28%), *Oceanobacillus* (13%), *Thermobifida* (13%), *Actinomadura* (12%), *Bacillus* (11%), and *Geobacillus* (6%) [10,11]. *Geobacillus* spp. grow between 55 and 65 °C and have been extensively studied for bioremediation, bioproduction, and thermotolerant enzyme production [12]. Enzymes produced by *Geobacillus* spp. include glycoside hydrolases, lipases, and proteases [13]. The thermoalkaliphilic lipases Lip29, TA, and B78 from *Geobacillus* spp. exhibit good thermostability and are expected to be used in the detergent industry [14–16].

At present, all lipases that can be added to detergents are alkaline, and their optimum pH is 8.0–12.0 [17]. An ideal lipase for detergent addition should have the following characteristics: high activity, high reaction temperature, high pH, and strong resistance to alkali substances, organic solvents, metal ions, and other chemical substances [18]. In this study, a novel GDSL family lipase, LipGt6, was cloned and characterized from the thermophilic bacterium *G. thermoleovorans* H9. The purified recombinant LipGt6 was found to have optimal activity at 50 °C and pH 9.0 and be thermostable up to 70 °C. The potential of this enzyme as a detergent additive was initially evaluated.

2. Materials and Methods

2.1. Strains, Plasmids, and Chemicals

The thermophilic bacterium *G. thermoleovorans* H9 and the plasmid pET28a were maintained in our laboratory. *E. coli* BL21-codonplus (DE3), DNA polymerase, and recombinase were purchased from Vazyme (Nanjing, China). Restriction endonucleases were purchased from NEB(Beverly, MA, USA), and all chemicals used in this study were of reagent grade.

2.2. Homology Modelling and Sequence Alignment

A 3D structural model was generated using SWISS-MODEL (https://swissmodel.expasy.org) (accessed on 12 March 2024). The PyMOL Molecular Graphics System (Version 3.0, Schrödinger, LLC, San Francisco, CA, USA) was subsequently used to analyze the tertiary structure of the lipase. To compare the conserved amino acid sequences, the peptide sequences of the bacterial esterases/lipases containing GDSL motifs were searched in NCBI (https://www.ncbi.nlm.nih.gov/taxonomy) (accessed on 12 March 2024) and PDB (http://www.rcsb.org/pdb/) (accessed on 12 March 2024). Secondary structure alignment was conducted using ClustalW [19], and alignment analysis was performed with ESPript3 [20].

2.3. Construction of the Expression Vector

The genome of *G. thermoleovorans* H9 was used as a DNA template, and the gene *LipGt6* was amplified by PCR with the following primers: LipGt6_F (5′ to 3′: cagcaaatgggtcgcg-gatccTTGTTGTGCTGCTGCTGGCTGC) and LipGt6_R (5′ to 3′: tggtggtgctcgagtgcggc-cgcTTGCAATAAGCTCCCTACCCA), which contained BamHI and NotI restriction sites, respectively. The amplified fragments were cloned and inserted into a pET-28a expression vector (Novagen) containing a C-terminal His-tag using a ClonExpress Ultra One Step Cloning Kit (Vazyme, Nanjing, China). The correct recombinant plasmids were transformed into *E. coli* BL21-codonplus (DE3) competent cells for gene expression.

2.4. Expression and Purification of LipGt6

The recombinant *E. coli* strains were subsequently grown overnight at 37 °C in LB supplemented with kanamycin (50 μg/mL). The cultured cells (3 mL) were transferred to 300 LB media supplemented with kanamycin and left at 37 °C until an optical density (0.6–0.8, at 600 nm) was reached. The cells were induced with 0.5 mM isopropyl β-D-1-thiogalactopyranoside (IPTG), and the cultures were incubated with shaking at 16 °C for 12 h. The cells were harvested by centrifugation at 8000× *g* for 10 min and resuspended in Tris-HCl (50 mM, pH 8.0). The bacteria were then disrupted by sonication and centrifuged at 10,000× *g* for 30 min at 4 °C, after which the supernatant was retained as a crude enzyme solution. The recombinant lipases were purified by nickel-nitrilotriacetic acid (Ni-NTA) affinity chromatography and eluted with an increasing imidazole gradient, and the target proteins were detected by sodium dodecyl sulfatepolyacrylamide gel electrophoresis (SDS-PAGE). The purified solution of LipGt6 was concentrated, and imidazole was removed by ultrafiltration with a 50 mM Tris-HCl (pH 8.0) buffer solution.

2.5. Substrate Specificity

Photometric assay was carried out according to Kordel et al. [21]. Solution A contained *p*NP esters with different lengths of acyl chains dissolved in 2-propanol, with a sonicator for 10 min at room temperature. Solution B was 50 mM Tris-HCI buffer (pH 9). A reaction mixture consisting of 1 part solution A and 10 parts solution B was prepared fresh before the assay. A 50 μL volume of an appropriate dilution of the enzyme solution was added to 575 μL of the reaction mixture, and 95% ethanol was added to stop the reaction. The kinetics were detected at 410 nm using a spectrophotometer. One unit of lipase activity was defined as the amount of enzyme that liberated 1 μmol of *p*-nitrophenol from substrate, respectively, per min.

The purified enzyme was mixed with substrate solutions that contained different lengths of acyl chains, including *p*-nitrophenyl acetate (pNPC2), *p*-nitrophenyl butyrate (*p*NPC4), *p*-nitrophenyl caprylate (*p*NPC8), *p*-nitrophenyl decanoate (*p*NPC10), *p*-nitrophenyl laurate (*p*NPC12), *p*-nitrophenyl myristate (*p*NPC14), *p*-nitrophenyl palmitate (*p*NPC16), and *p*-nitrophenyl stearate (*p*NPC18) at 50 °C and 50 mM Tris-HCl (pH 9.0). The highest degrading enzyme activity, *p*NP-C8 enzyme activity, was defined as 100%, and relative comparative analyses of enzyme activities for other substrate degradations were conducted.

2.6. Effects of Temperature and pH on Enzyme Activity and Stability

The optimum temperature was determined by testing temperatures between 30 and 90 °C using *p*NPC8 at pH 9. The optimum pH value between pH 6 and 11 was evaluated with *p*NPC8 at 50 °C. Reactions were performed in 0.1 M citric acid-Na_2HPO4 (pH 5–7) and 0.1 M Tris-HCl (pH 7–10) buffers. The effect of temperature on LipGt6 stability was determined at various temperatures (50–80 °C) for 3 h, followed by a residual enzyme activity assay at 50 °C and pH 9 Tris-HCl. The impact of pH on LipGt6 stability was determined by incubating the samples at pH 6–11 for 1 h at 50 °C followed by a residual enzyme activity assay at 50 °C and pH 9. The optimum temperature, pH, and pH stability of LipGt6 were determined, and the relative enzyme activity was calculated using the highest enzyme activity as 100%. The temperature stability of LipGt6 was determined, and the relative enzyme activity for other incubation times was calculated using the initial enzyme activity as 100%.

2.7. Effects of Metal Ions, Surfactants, and Oxidizing Agents on Enzyme Activity

LipGt6 was subjected to activity assays after treatment with 5 mM metal ions (Zn^{2+}, Mg^{2+}, Ca^{2+}, Mn^{2+}, Cu^{2+}, Ni^{2+}, Fe^{2+}, and Na^{+}) for 1 h at 50 °C. The influence of detergents on LipGt6 activity was assayed by adding 1 mM sodium dodecyl sulfate (SDS), 1% (*v*/*v*) Tween-20, Tween-80, Triton X-100, and sodium deoxycholate to the reaction solutions for 1 h at 50 °C. The enzymes were incubated with different concentrations of H_2O_2 and NaClO (1–5%) at 50 °C for 1 h, and the enzyme stability was determined according to the residual

enzyme activity. The activity of the enzyme was calculated after 1 h of incubation, using the untreated enzyme activity as 100%.

2.8. Site-Directed Mutagenesis

Based on multiple sequence comparisons, the predicted catalytic activity sites were mutated to alanine acid using a Fast Mutagenesis Kit (Vazyme, Nanjing, China) according to the manufacturer's instructions. A wild-type plasmid was used as a template to expand plasmids with primers containing mutant nucleotides. The primer pairs utilized are listed in Table S1. All mutation sites were confirmed by DNA sequencing, and the mutant plasmids were transformed into *E. coli* BL21-codonplus (DE3) cells for expression. The enzymatic activity of the mutant strains was detected as described above. The negative control was the enzyme inactivated at high temperature.

2.9. Statistical Analysis

The results were analyzed using one-way ANOVA with SPSS Statistics 25 software (IBM SPSS Statistics, Armonk, NY, USA) in a completely randomized design. The results were analyzed with GraphPad Prism 8.0.2 (GraphPad Software, San Diego, CA, USA), and error bars represent standard deviation. Differences in means between groups were compared for statistical significance at $p < 0.05$.

3. Results

3.1. Sequence Analysis of the Enzyme LipGt6

A putative lipase was found in the genome sequence of *G. thermoleovorans* H9, designated LipGt6, which is composed of 762 nucleotides that correspond to 254 amino acids. A conserved domain search of LipGt6 from NCBI revealed that LipGt6 contains the SGNH-hydrolase YpmR-like domain, which belongs to the GDSL family of lipases/esterases. BLASTP analysis revealed over 90% identity matches for LipGt6 with various GDSL family lipases/esterases belonging to *Geobacillus* spp., such as the hydrolase protein of *Geobacillus* sp. JS12 (96.85%). Selected typical lipolytic enzyme sequences with GDSL motifs were subjected to multiple sequence alignments. LipGt6 possesses a conserved GDSL motif near the N-terminus, and four invariant important catalytic residues, Ser, Gly, Asn, and His in blocks I, II, III, and V, respectively, which are essential for the enzyme to perform its catalytic function (Figure 1). The serine residue acts as a nucleophilic reagent and proton donor for the oxyanion hole, while histidine increases the nucleophilicity of serine residues by deprotonation [22].

3.2. Cloning, Expression, and Purification of LipGt6

The LipGt6 gene was inserted into pET-28a, and constructed plasmids with an N-terminal His-tag were transformed into *E. coli* BL21-codonplus (DE3). Then, 0.5 mM IPTG was used to express the recombinant LipGt6 protein, which was successfully purified by nickel affinity chromatography, as verified by SDS-PAGE (Figure 2). The purified enzyme showed a single band on SDS-PAGE with a molecular mass of approximately 28 kDa, at 50 mM and 100 mM imidazole.

3.3. Substrate Specificity of LipGt6

The substrate specificity of LipGt6 was determined by using *p*NP esters of different chain lengths as substrates. Recombinant LipGt6 exhibited the highest activity towards medium- and long-chain fatty acids, followed by *p*NP-C8, *p*NP-C10, *p*NP-C12, and *p*NP-C14, and some degradation activity towards *p*NP-C16 and *p*NP-C18; therefore, LipGt6 is a lipase, not an esterase (Figure 3). The purified enzyme LipGt6 exhibited a specific enzyme activity of 10.87 U/mg using *p*NPC8 substrate. After purification treatment, the enzyme showed 3.59-time purification.

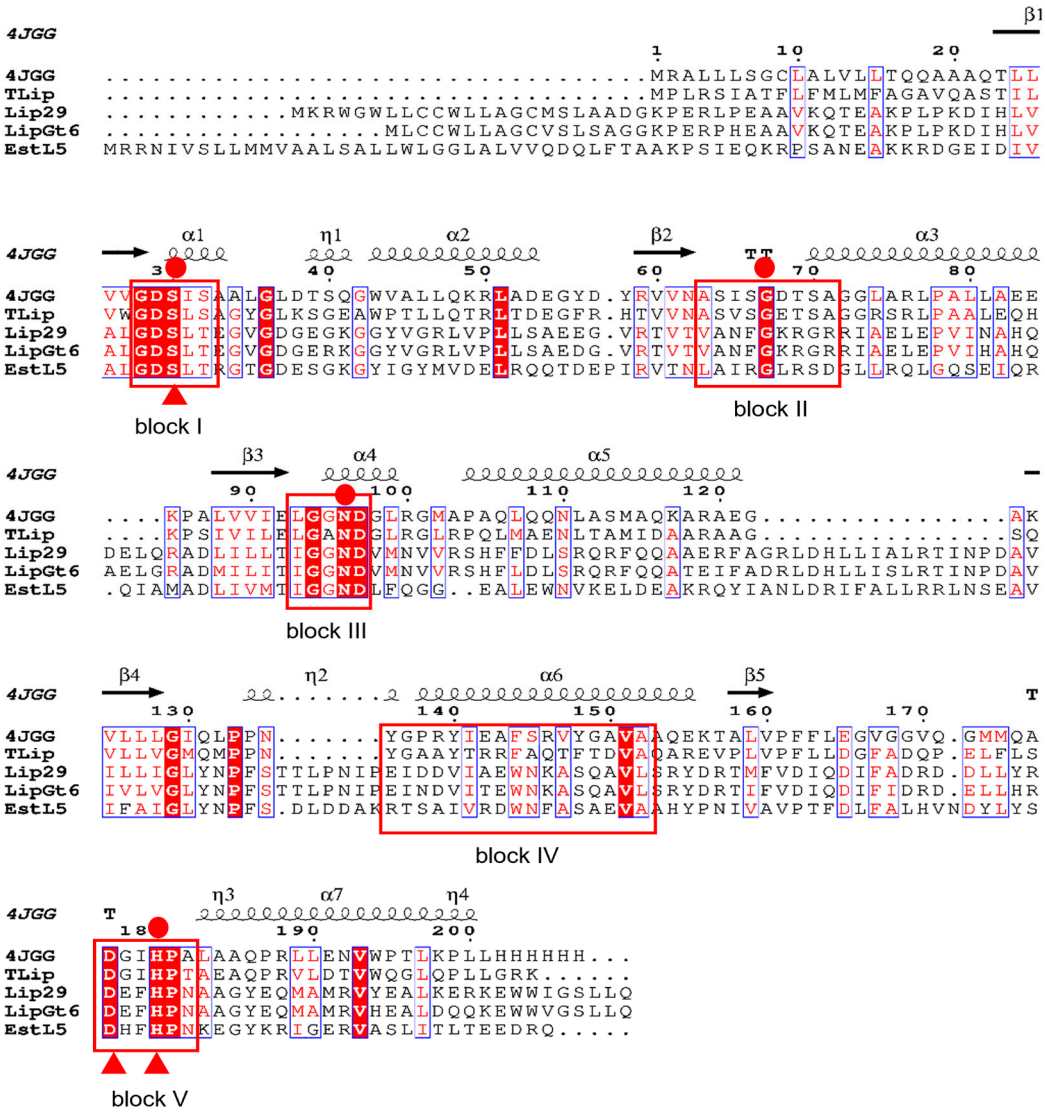

Figure 1. Multiple sequence alignment of LipGt6 with other GDSL families of esterases and lipases. Secondary structures including α-helices and β-sheets are shown based on PDB 4JGG. The five conserved blocks of I, II, III, IV, and V are boxed. Closed triangles indicate amino acid residues that are conserved in the catalytic triad. Closed circles represent four invariant important catalytic residues. 4JGG: GDSL-family lysophospholipase of *Pseudomonas aeruginosa*; TLip: arylesterase of *Thauera* sp. (Accession No. WP_038010598); Lip29: GDSL-family lipase of *Geobacillus thermoleovorans* (Accession No. ASS99449.1); EstL5: GDSL-family esterase of *Geobacillus thermodenitrificans* T2 (Accession No. ACD02023).

3.4. Effects of Temperature and pH on LipGt6

The temperature and pH tolerance of the recombinant LipGt6 were determined using *p*NP-C8 as the substrate. LipGt6 showed optimum activity at pH 9 in Tris-HCl and maintained more than 75% of its activity at pH 8 and 10. Enzyme activity was not affected when LipGt6 was incubated in Tris-HCl at pH 9–10 for 1 h (Figure 4a,c). In Tris-HCl at pH 9, the maximum enzyme activity was observed for purified LipGt6 at 50 °C, and the enzyme maintained more than 90% of its activity at 40 to 70 °C (Figure 4b). LipGt6 was incubated at 50 °C, 60 °C, and 70 °C for 3 h, and the enzyme was stable without any significant loss of activity. However, the stability of LipGt6 sharply decreased at temperatures above 80 °C, and approximately 40% of the residual activity was maintained after 1 h (Figure 4d).

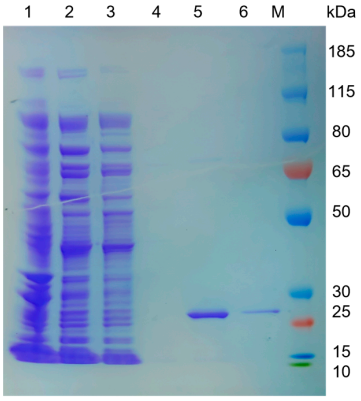

Figure 2. SDS-PAGE analysis of recombinant LipGt6. Lane M: standard protein molecular mass markers; lane 1: crude enzyme extract; lanes 2: flow-through fraction; lanes 3, 4, 5, and 6: elution fractions with 5, 10, 50, and 100 mM imidazole, respectively.

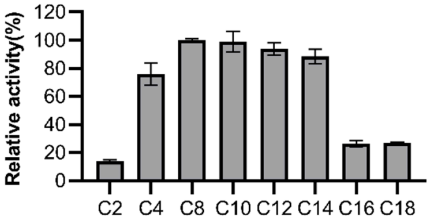

Figure 3. Substrate specificity of recombinant LipGt6. Reactions were incubated at 50 °C with 50 mM Tris-HCl buffer, pH 9.0. C2, *p*NP-C2; C4, *p*NP-C4; C8, *p*NP-C8; C10, *p*NP-C10; C12, *p*NP-C12; C14, *p*NP-C14; C16, *p*NP-C16; C18, *p*NP-C18. Data points are the average of triplicate experiments, and the bars indicate the standard deviations.

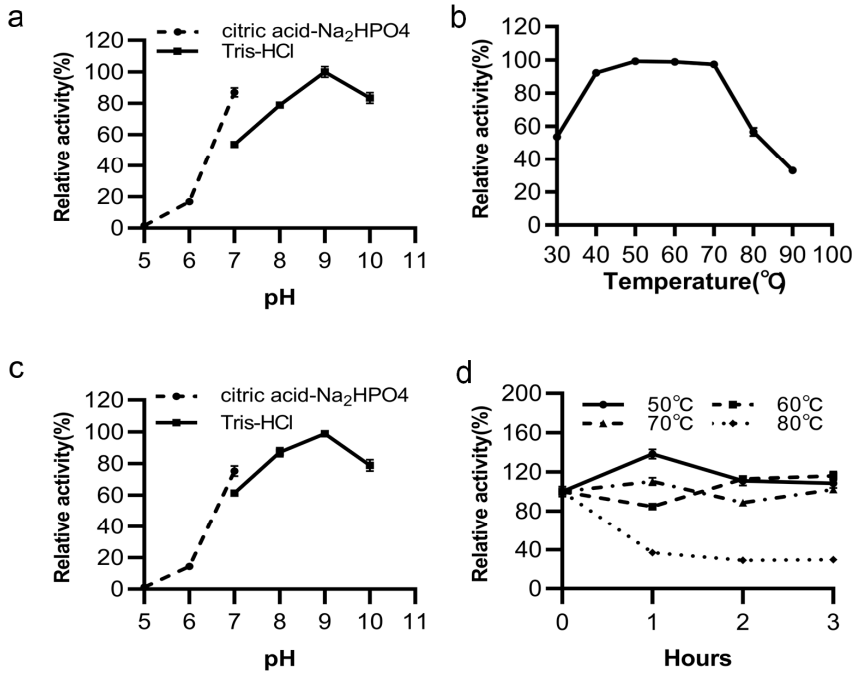

Figure 4. Effects of pH and temperature on the activity of recombinant LipGt6. (**a**) Effects of pH on the activity of LipGt6 using *p*NP-C8 as a substrate. (**b**) Effects of temperature on the activity of LipGt6 using *p*NP-C8 as a substrate. (**c**) Effect of pH on the stability of LipGt6 using *p*NP-C8 as a substrate. (**d**) Effects of temperature on the stability of LipGt6 using *p*NP-C8 as a substrate. The data points in Figure 4 are the average of triplicate experiments, and the error bars represent the standard deviation.

3.5. Effects of Metal Ions, Surfactants, and Oxidizing Agents on LipGt6

The effect of metal ions and detergents on enzyme activity was determined using *p*NP-C8 as a substrate. At 5 mM, the metal ions Mg^{2+}, Mn^{2+}, Ca^{2+}, and Na^{+} activate the enzyme. LipGt6 activity was significantly inhibited by Zn^{2+}, Ni^{2+}, Cu^{2+}, and Fe^{2+} (Figure 5). LipGt6 was compatible with the following surfactants: SDS and Triton X-100. In the presence of 1% H_2O_2 and sodium deoxycholate, LipGt6 retained 70 to 75% relative activity, but incubation with Tween 20 or Tween 80 for 1 h significantly reduced the enzyme activity, as 30% of the activity remained (Table 1).

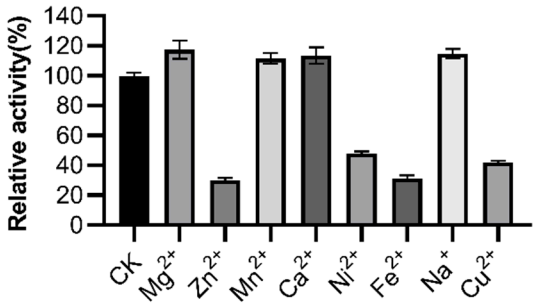

Figure 5. Effects of metal ions on LipGt6 activity. The enzyme was subjected to activity assays after treatment with 5 mM metal ions (Zn^{2+}, Mg^{2+}, Ca^{2+}, Mn^{2+}, Cu^{2+}, Ni^{2+}, Fe^{2+}, and Na^{+}) for 1 h at 50 °C. The relative activity of the control without metal ions was regarded as 100%. Data points are the average of triplicate experiments, and error bars represent standard deviation.

Table 1. Effects of surfactants and other chemical reagents on LipGt6.

Chemical Reagents	Relative Activity (%)
CK	100.00 ± 3.93
1 mM SDS	40.05 ± 1.94
1% Triton X-100	41.70 ± 2.18
1% Tween-80	28.03 ± 1.55
1% Tween-20	29.26 ± 1.68
1% sodium deoxycholate	75.72 ± 5.76
1% H_2O_2	69.50 ± 16.61
5% NaClO	4.09 ± 0.17
1% NaClO	10.70 ± 0.18

3.6. Analysis of the LipGt6 Catalytic Triad

An esterase from *G. thermodenitrificans* (PDB: 7E16), a member of the GDSL hydrolase family with 32.06% amino acid sequence homology to LipGt6, was used to construct the LipGt6 model. The structural model of LipGt6 shows five central β-sheet structures surrounded by nine α-helices. The predicted catalytic triad that contains serine, aspartate, and histidine is clearly present on the surface mode structure (Figure 6a). To confirm that the predicted catalytic triad was the actual active site, site-directed mutagenesis was used to substitute these three amino acid residues of the catalytic triad (Ser47, Asp221, and His224) with alanine. The engineered proteins were overexpressed in *E. coli* BL21-codonplus (DE3) cells, and the residual enzyme activity of the mutants was assayed after the proteins were purified by Ni-affinity chromatography (Figure 6b). The reported catalytic triad of the GDSL family lipase Lip29 consists of Ser53, His230, and Asp227, which are commonly conserved residues [14]. LipGt6 exhibited less than 20% activity after mutation of Ser47 and His224, and mutation of Asp221 did not affect the activity. *Bacillus* sp. K91 encodes Est8, an esterase with reduced activity upon mutation of Ser, Asp, and His residues, while still retaining detectable activity [23]. Based on the results obtained with this mutation, the catalytic residues Ser and His of LipGt6 were more critical than Asp. The potential catalytic triad found in known GDSL lipases may not be the critical amino acid that participates in

the lipolytic reaction of LipGt6. The specific lipolytic activity of LipGt6 may involve an unknown catalytic motif.

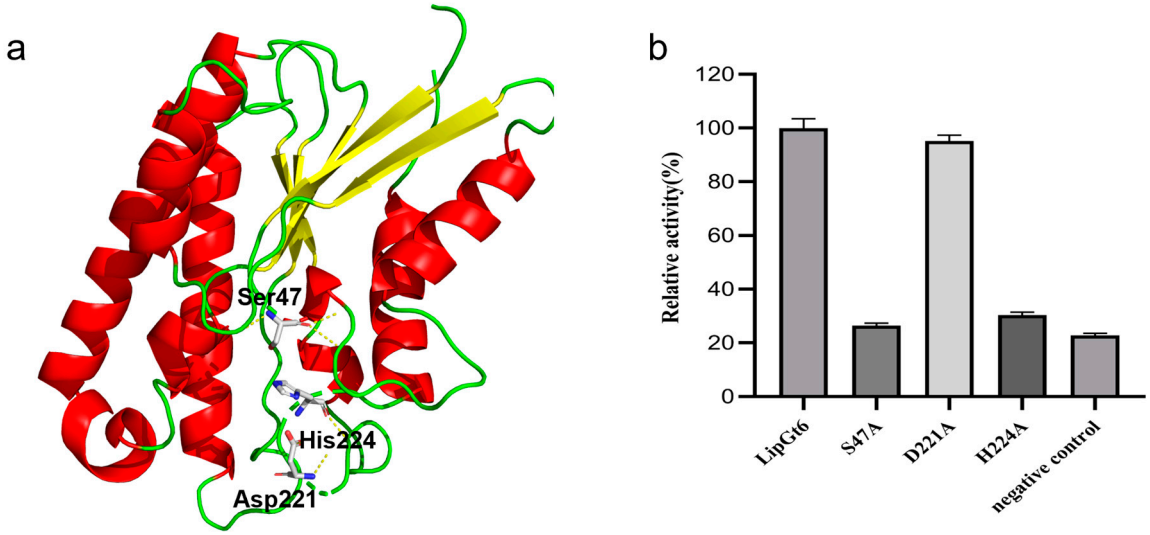

Figure 6. Three-dimensional modelling and mutant activity of LipGt6. (**a**) The tertiary structure of LipGt6 was modelled based on that of an esterase from *G. thermodenitrificans* (PDB: 7E16). The catalytic triads are shown (Ser47, Asp221, His224). The β-sheet structures and α-helices are colored yellow and red, respectively. (**b**) Retention enzyme activity of the S47A, D221A, and H224A mutants. Data points in Figure 6b are the average of triplicate experiments, and error bars represent the standard deviation.

4. Discussion

Due to their biotechnological potential, lipolytic enzymes are attracting enormous attention [24,25]. Most lipases used in industry are microbial enzymes that originate from fungal or bacterial sources. Bacterial lipolytic enzymes II family are widespread, display broad substrate specificities, and have a diverse range of hydrolytic functions, such as carboxylesterase, lipase, protease, thioesterase, lysophospholipase, and acyltransferases activities [22]. Numerous family II esterases have been characterized. The thermophilic bacterium *Bacillus* sp. K91 encodes an esterase, Est19, which is highly stable in alkaline solutions, denaturants, and detergents; is stable at 60 °C; and has deacetylase activity in semisynthetic antibiotics [26]. Recombinant EstL5 from *G. thermodenitrificans* T2 was characterized. EstL5 displayed 24% of its highest activity at 0 °C and exhibited a unique cold-adaptation feature [27,28]. A novel GDSL esterase J15 was activated by Tween-20, -60, and Triton X-100 and inhibited by 1 mM SDS [29]. To date, there have been few reports on the natural characteristics and structural features of GDSL family lipases. In this study, LipGt6, a new thermophilic lipase, from *G. thermoleovorans* H9, was cloned, purified, and characterized. The sequences were processed using DNAMAN Version 6.0 (Lynnon Biosoft, San Ramon, CA, USA). LipGt6 has 85.77% similarity with *G. thermocatenulatus* Lip29 [14]. However, they have different substrate preferences. Lip29 exhibited the maximum activity towards long-chain fatty acids (C12–C16) and almost no activity towards short-chain fatty acids. The recombinant LipGt6 exhibited the highest activity towards medium- and long-chain fatty acids (C8–C14). LipGt6 has 12.6% sequence similarity with the lipase Lip486 [17]. Both Lip29 and Lip486 are reported lipases that belong to the GDSL family.

Sequence comparison analysis of LipGt6, a GDSL family lipase, revealed a Gly-Asp-Ser-(Leu) [GDS(L)] motif that contained an active-site serine residue. Site-directed mutagenesis was used to substitute these three amino acid residues of the catalytic triad (Ser47, Asp221, and His224) with alanine. The activity of the D221A mutant was unaffected, whereas the activity of the S47A and H224A mutants was the same as that of the negative control, indicating that the S47A and H224A mutants were inactive. Typically, the

catalytic triad involves a histidine, an aspartic residue that lies three positions upstream of the active-site histidine, and an important serine [30], as observed in *G. thermocatenulatus* Lip29 [14] and *Bacillus* sp. Est19 [26]. Brumlik and Buckley [31] proposed that the aspartic acid residue is Asp-116, which is located in block III, and the catalytic triad of the enzyme consists of Ser-16, Asp-116, and His-291. The specific lipolytic activity of LipGt6 may involve an unknown catalytic motif. More structural information is needed to establish whether LipGt6 proteins share a common architecture of their catalytic triad (or dyad) in addition to the similarity of their sequences [32].

In this study, the lipase LipGt6 had a molecular weight of 28 kDa, and its optimal temperature and pH were 50 °C and 9.0, respectively. The enzyme was also thermostable up to 70 °C. Optimum temperature and pH for *Bacillus stearothermophilus* P1 lipase were 55 °C and pH 8.5 and it was highly stable in the temperature range of 30–65 °C [33]. Lee et al. purified two thermostable lipases (A and B) from *Bacillus thermooleovorans* ID-1 [34]. Lipase A and B have optimal temperatures of 60–65 °C and 60 °C, respectively, while the pH optima were 9 and 8–9, respectively. The detergent industry is an important application field for lipase. Surfactants and oxidants play a major role in detergents. Generally, the surfactant has negative effects on enzymatic hydrolysis and acts as a competitive inhibitor in the reaction system. The detergent lipases must be highly tolerant to surfactants and detergent additives. In the presence of 1% detergents such as Tween-20 and sodium deoxycholate, lipase P1 showed 14% and 42% relative activity, respectively [33]. LipGt6 retained 30% and 75% relative activity, respectively. In addition, it was reported that 0.1–1% H_2O_2 completely inhibits the *B. smithii* lipase [35]. In the presence of 1% H_2O_2, LipGt6 retained 69.5% relative activity. Therefore, it has good application prospects in the detergent industry.

Researchers have suggested that the change in lipase activity may result from a conformational change in the interaction between lipase and metal ions [36]. The L1 lipase structure shows a novel zinc-coordinated extra domain that is conserved among members of the lipase family I.5. The novel zinc site stabilizes the structural domain by coordinating with His-81, Asp-61, and Asp-238. Calcium-dependent stability has been demonstrated by Kim et al.; lipase L1 begins to unfold at 66 °C in the presence of calcium ions but at 58 °C in the absence of calcium. The residues of the Ca^{2+}-binding site are located near the catalytic His and Asp residues, stabilizing the active center of these enzymes [37]. Many of the lipases were activated when Ca^{2+} and Mg^{2+} were added [38,39]. LipGt6 enzyme activity was increased in the presence of 5 mM Mg^{2+} (117.49%) and Ca^{2+} (113.50%). However, no similar calcium-binding site has been reported in the lipase II family. Further structural information and experimental data are required to determine whether there are related residues.

5. Conclusions

The thermophilic lipase LipGt6, which belongs to the GDSL hydrolase family, was cloned and characterized in this work. The enzyme exhibited the highest activity against medium- and long-chain fatty acids and showed high stability in alkaline solutions, at 70 °C, and in the presence of detergents and oxidizing agents, which is important for its application as a detergent additive. The biochemical functions (structure-function relationships) of many GDSL family lipases remain unknown and should be further investigated.

Supplementary Materials: The following supporting information can be downloaded at: https://www.mdpi.com/article/10.3390/app14083279/s1. Table S1: Primers used in this study.

Author Contributions: Conceptualization: L.Q., J.W. and M.L.; methodology: L.Q. and Y.Z.; validation: L.Q.; formal analysis and investigation: L.Q. and Z.Z.; resources: Z.Z. and J.W.; data curation: L.Q. and S.J.; writing—original draft preparation: L.Q.; writing—review and editing: L.Q., Z.Z. and S.J.; supervision and project administration: M.L. and J.W.; funding acquisition: M.L., Z.Z. and Y.Z. All authors have read and agreed to the published version of the manuscript.

Funding: This research was funded by the National Key R&D Program of China (2023YFF1000300, 2023YFF1000304), the Third Xinjiang Scientific Expedition (2022xjkk020602), the National Natural Science Foundation of China (32150021, 32370091), and the Agricultural Science and Technology Innovation Program of the Chinese Academy of Agricultural Sciences (CAAS-ZDRW202305).

Institutional Review Board Statement: Not applicable.

Informed Consent Statement: Not applicable.

Data Availability Statement: Data are contained within the article and Supplementary Materials.

Acknowledgments: Special thanks go to Wei Lu for their constructive suggestions on the revision of the article and other authors for their excellent technical support.

Conflicts of Interest: The authors declare no conflicts of interest.

References

1. Patel, N.; Rai, D.; Shivam; Shahane, S.; Mishra, U. Lipases: Sources, Production, Purification, and Applications. *Recent Pat. Biotechnol.* **2019**, *13*, 45–56. [CrossRef] [PubMed]
2. Melani, N.B.; Tambourgi, E.B.; Silveira, E. Lipases: From production to applications. *Sep. Purif. Rev.* **2020**, *49*, 143–158. [CrossRef]
3. Hitch, T.C.A.; Clavel, T. A proposed update for the classification and description of bacterial lipolytic enzymes. *PeerJ* **2019**, *7*, e7249. [CrossRef] [PubMed]
4. Mlgaard, A.; Kauppinen, S.; Larsen, S. Rhamnogalacturonan acetylesterase elucidates the structure and function of a new family of hydrolases. *Structure* **2000**, *8*, 373–383. [CrossRef] [PubMed]
5. Bharathi, D.; Rajalakshmi, G. Microbial lipases: An overview of screening, production and purification. *Biocatal. Agric. Biotechnol.* **2019**, *22*, 101368. [CrossRef]
6. Abdella, B.; Youssif, A.M.; Sabry, S.A.; Ghozlan, H.A. Production, purification, and characterization of cold-active lipase from the *psychrotroph Pseudomonas* sp. A6. *Braz. J. Microbiol.* **2023**, *54*, 1623–1633. [CrossRef]
7. Li, J.; Shen, W.; Fan, G.; Li, X. Screening, purification and characterization of lipase from *Burkholderia pyrrocinia* B1213. *3 Biotech* **2018**, *8*, 1–12. [CrossRef]
8. Cho, A.-R.; Yoo, S.-K.; Kim, E.-J. Cloning, sequencing and expression in Escherichia coli of a thermophilic lipase from *Bacillus thermoleovorans* ID-1. *FEMS Microbiol. Lett.* **2000**, *186*, 235–238. [CrossRef]
9. Bacha, A.B.; Moubayed, N.M.S.; Abid, I. Thermostable, alkaline and detergent-tolerant lipase from a newly isolated thermophilic *Bacillus stearothermophilus*. *Indian J. Biochem. Biophys.* **2015**, *52*, 179–188.
10. Cao, Y.; Huang, H.; Qian, Y.; Wang, L.; Xu, Y.; Jin, H.; Sun, J.; Chang, Z. Hyperthermophilic pretreatment device and its application on improving decomposition effect for chicken manure and rice straw aerobic composting. *Trans. Chin. Soc. Agric. Eng.* **2017**, *33*, 243–250.
11. Yu, Z.; Zhou, S. Hyperthermophilic composting of organic solid wastes: Accelerated humification and pollution control mechanisms. *J. Nanjing Agric. Univ.* **2020**, *43*, 781–789.
12. Burgess, S.; Flint, S.; Lindsay, D.; Cox, M.; Biggs, P. Insights into the *Geobacillus stearothermophilus* species based on phylogenomic principles. *BMC Microbiol.* **2017**, *17*, 140. [CrossRef] [PubMed]
13. Wang, M.; Zhu, H.; Kong, Z.; Li, T.; Ma, L.; Liu, D.; Shen, Q. Pan-Genome Analyses of *Geobacillus* spp. Reveal Genetic Characteristics and Composting Potential. *Int. J. Mol. Sci.* **2020**, *21*, 3393. [CrossRef]
14. Jo, E.; Kim, J.; Lee, A.; Moon, K.; Cha, J. Identification and Characterization of a Novel Thermostable GDSL-Type Lipase from *Geobacillus thermocatenulatus*. *J. Microbiol. Biotechnol.* **2021**, *31*, 483–491. [CrossRef]
15. Abol-Fotouh, D.; AlHagar, O.E.; Hassan, M.A. Optimization, purification, and biochemical characterization of thermoalkaliphilic lipase from a novel *Geobacillus stearothermophilus* FMR12 for detergent formulations. *Int. J. Biol. Macromol.* **2021**, *181*, 125–135. [CrossRef]
16. Bayoumi, R.A.; El-Louboudey, S.S.; Sidkey, N.M.; Abd-El-Rahman, M.A. Production, Purification and Characterization of Thermoalkalophilic Lipase for Application in Bio-detergent Industry. *J. Appl. Sci. Res.* **2007**, *3*, 1752–1765.
17. Xiao, Y.; Liu, Y.-D.; Yuan, G.; Mao, R.-Q.; Li, G. An uncharacterized protein from the metagenome with no obvious homology to known lipases shows excellent alkaline lipase properties and potential applications in the detergent industry. *Biotechnol. Lett.* **2021**, *43*, 2311–2325. [CrossRef]
18. Salihu, A.; Alam, M.Z. Solvent tolerant lipases: A review. *Process Biochem.* **2015**, *50*, 86–96. [CrossRef]
19. Thompson, J.D.; Higgins, D.G.; Gibson, T.J. CLUSTAL W: Improving the sensitivity of progressive multiple sequence alignment through sequence weighting, position-specific gap penalties and weight matrix choice. *Nucleic Acids Res.* **1994**, *22*, 4673–4680. [CrossRef]
20. Robert, X.; Gouet, P. Deciphering key features in protein structures with the new ENDscript server. *Nucleic Acids Res.* **2014**, *42*, W320–W324. [CrossRef]
21. Kordel, M.; Hofmann, B.; Schomburg, D.; Schmid, R.D. Extracellular lipase of *Pseudomonas* sp. strain ATCC 21808: Purification, characterization, crystallization, and preliminary X-ray diffraction data. *J. Bacteriol.* **1991**, *173*, 4836–4841. [CrossRef] [PubMed]

22. Akoh, C.C.; Lee, G.-C.; Liaw, Y.-C.; Huang, T.-H.; Shaw, J.-F. GDSL family of serine esterases/lipases. *Prog. Lipid Res.* **2004**, *43*, 534–552. [CrossRef] [PubMed]
23. Ding, J.; Zhu, H.; Ye, Y.; Li, J.; Han, N.; Wu, Q.; Huang, Z.; Meng, Z. A thermostable and alkaline GDSL-motif esterase from *Bacillus* sp. K91: Crystallization and X-ray crystallographic analysis. *Acta Crystallogr. Sect. F Struct. Biol. Commun.* **2018**, *74*, 117–121. [CrossRef] [PubMed]
24. Jaeger, K.E.; Dijkstra, B.W.; Reetz, M.T. Bacterial Biocatalysts: Molecular Biology, Three-Dimensional Structures, and Biotechnological Applications of Lipases. *Annu. Rev. Microbiol.* **1999**, *53*, 315–351. [CrossRef] [PubMed]
25. Jaeger, K.-E.; Reetz, M. Microbial lipases form versatile tools for biotechnology. *Trends Biotechnol.* **1998**, *16*, 369–403. [CrossRef] [PubMed]
26. Yu, T.; Ding, J.; Zheng, Q.; Han, N.; Yu, J.; Yang, Y.; Li, J.; Mu, Y.; Wu, Q.; Huang, Z. Identification and characterization of a new alkaline SGNH hydrolase from a thermophilic bacterium *Bacillus* sp. K91. *J. Microbiol. Biotechnol.* **2016**, *26*, 730–738. [CrossRef]
27. Yang, Z.; Zhang, Y.; Shen, T.; Xie, Y.; Mao, Y.; Ji, C. Cloning, expression and biochemical characterization of a novel, moderately thermostable GDSL family esterase from *Geobacillus thermodenitrificans* T2. *J. Biosci. Bioeng.* **2013**, *115*, 133–137. [CrossRef] [PubMed]
28. Yang, Z.; Zhang, Y.; Qiu, R.; Huang, J.; Ji, C. Crystallization and preliminary X-ray diffraction analysis of a thermostable GDSL-family esterase, EstL5, from *Geobacillus thermodenitrificans* T2. *Acta Crystallogr.* **2013**, *69*, 776–778.
29. Abu, S.; Leow, B.; Chor, T.; Raja, R.; Zaliha, N. Cloning, expression and characterization of a novel cold-adapted GDSL family esterase from *Photobacterium* sp. strain J15. *Extrem. Life Under Extrem. Cond.* **2016**, *20*, 44–55.
30. Lescic Asler, I.; Stefanic, Z.; Mar?Avelski, A.; Vianello, R.; Kojic-Prodic, B. Catalytic Dyad in the SGNH Hydrolase Superfamily: In-depth Insight into Structural Parameters Tuning the Catalytic Process of Extracellular Lipase from *Streptomyces rimosus*. *ACS Chem. Biol.* **2017**, *12*, 1928–1936. [CrossRef]
31. Brumlik, M.J.; Buckley, J.T. Identification of the catalytic triad of the lipase/acyltransferase from *Aeromonas hydrophila*. *J. Bacteriol.* **1996**, *178*, 2060–2064. [CrossRef] [PubMed]
32. Arpigny, J.L.; Jaeger, K.E. Bacterial lipolytic enzymes: Classification and properties. *Biochem. J.* **1999**, *343*, 177–183. [CrossRef] [PubMed]
33. Sinchaikul, S.; Sookkheo, B.; Phutrakul, S.; Pan, F.-M.; Chen, S.-T. Optimization of a thermostable lipase from *Bacillus stearothermophilus* P1: Overexpression, purification, and characterization. *Protein Expr. Purif.* **2001**, *22*, 388–398. [CrossRef] [PubMed]
34. Lee, D.-W.; Kim, H.-W.; Lee, K.-W.; Kim, B.-C.; Choe, E.-A.; Lee, H.-S.; Kim, D.-S.; Pyun, Y.-R. Purification and characterization of two distinct thermostable lipases from the gram-positive thermophilic bacterium *Bacillus thermoleovorans* ID-1. *Enzym. Microb. Technol.* **2001**, *29*, 363–371. [CrossRef]
35. Lailaja, V.; Chandrasekaran, M. Detergent compatible alkaline lipase produced by marine *Bacillus smithii* BTMS 11. *World J. Microbiol. Biotechnol.* **2013**, *29*, 1349–1360. [CrossRef] [PubMed]
36. Zhao, J.; Ma, M.; Zeng, Z.; Yu, P.; Deng, S. Production, purification and biochemical characterisation of a novel lipase from a newly identified lipolytic bacterium *Staphylococcus caprae* NCU S6. *J. Enzym. Inhib. Med. Chem.* **2021**, *36*, 248–256. [CrossRef] [PubMed]
37. Kim, K.K.; Song, H.K.; Shin, D.H.; Hwang, K.Y.; Suh, S.W. The crystal structure of a triacylglycerol lipase from *Pseudomonas cepacia* reveals a highly open conformation in the absence of a bound inhibitor. *Structure* **1997**, *5*, 173–185. [CrossRef] [PubMed]
38. Khan, M.; Jithesh, K. Expression and purification of organic solvent stable lipase from soil metagenomic library. *World J. Microbiol. Biotechnol.* **2012**, *28*, 2417–2424. [CrossRef]
39. Zheng, J.; Liu, C.; Liu, L.; Jin, Q. Characterisation of a thermo-alkali-stable lipase from oil-contaminated soil using a metagenomic approach. *Syst. Appl. Microbiol.* **2013**, *36*, 197–204. [CrossRef]